

BBDEV. MEMO #019
2008 June 8

To: VLBI2010 Broadband Development Group
From: Brian Corey
Subject: Preliminary analysis of correlator data from 2008 May 23 GGAO-Westford BBD test

Summary of main conclusions:

1. When the correlator data are fringe-fit with manual phases, the stability of the fringe phase and multiband delay differences between polarizations is excellent.
2. When phase cal is used in the fringe-fitting, the stability of the multiband delay differences is poor, and there are large variations in fringe phase over frequency.
3. The lack of any detections for one of the cross-hands is difficult to explain.

1. Some salient facts about the data acquisition, correlation, and notation

- Both stations used new wideband dual-pol receivers, UDCs, DBEs, and Mark5Bs.
- Eight 32-MHz-wide channels spaced 64 MHz apart between 8.6 and 9.1 GHz were 2-bit sampled and recorded as LSB baseband channels for both linear polarizations.
- Data were recorded on source 3C84 from 1640 to 1900 UT, in scans that started on the 10-minute marks and lasted 9 minutes 30 seconds each.
- High yield from the initial parallel- and cross-hands correlation was obtained on 12 scans. Due to a problem with one of the GGAO disks, scan 144-1730 produced less than one minute of data and is used in this memo only for its phase cal data. Scan 144-1820 yielded no data in the initial correlation; recorrelation on June 5 was fully successful but occurred too late to be included in this memo.
- For historical reasons, polarization sense is labeled R or L at the correlator, and therefore also in this memo, even though the feeds are nominally sensitive to linear pol H and V. The mapping is $L \leftrightarrow V$ and $R \leftrightarrow H$.
- Correlation polarizations are referred to as LL, RR, LR, and RL, where the first character indicates the polarization at Westford and the second the polarization at GGAO.
- Fringes were detected in all 12 scans for LL, RR, and LR, but in no scans for RL. SNRs for the detections ranged from 7.6 to 84 when manual phases were used in fringe-fitting, with a general trend of increasing SNR over time.

2. Fringe-fitting method and multiband delays

The correlator data were initially fringe-fit using the phases of the 4.0-MHz-baseband phase cal (pcal) tones extracted from the recorded data to adjust the cross-correlation phases in the

individual frequency channels. It was apparent from the higher-SNR scans that the pcal phases did a poor job of aligning the fringe phases over frequency – see the “fringe phase” curves in the lower panels of figure 1. For comparison, the pcal phase differences between the two stations are also shown. Note the striking similarity between each pair of curves. The pcal phases are introducing a strong frequency dependence into the pcal-“corrected” fringe phases.

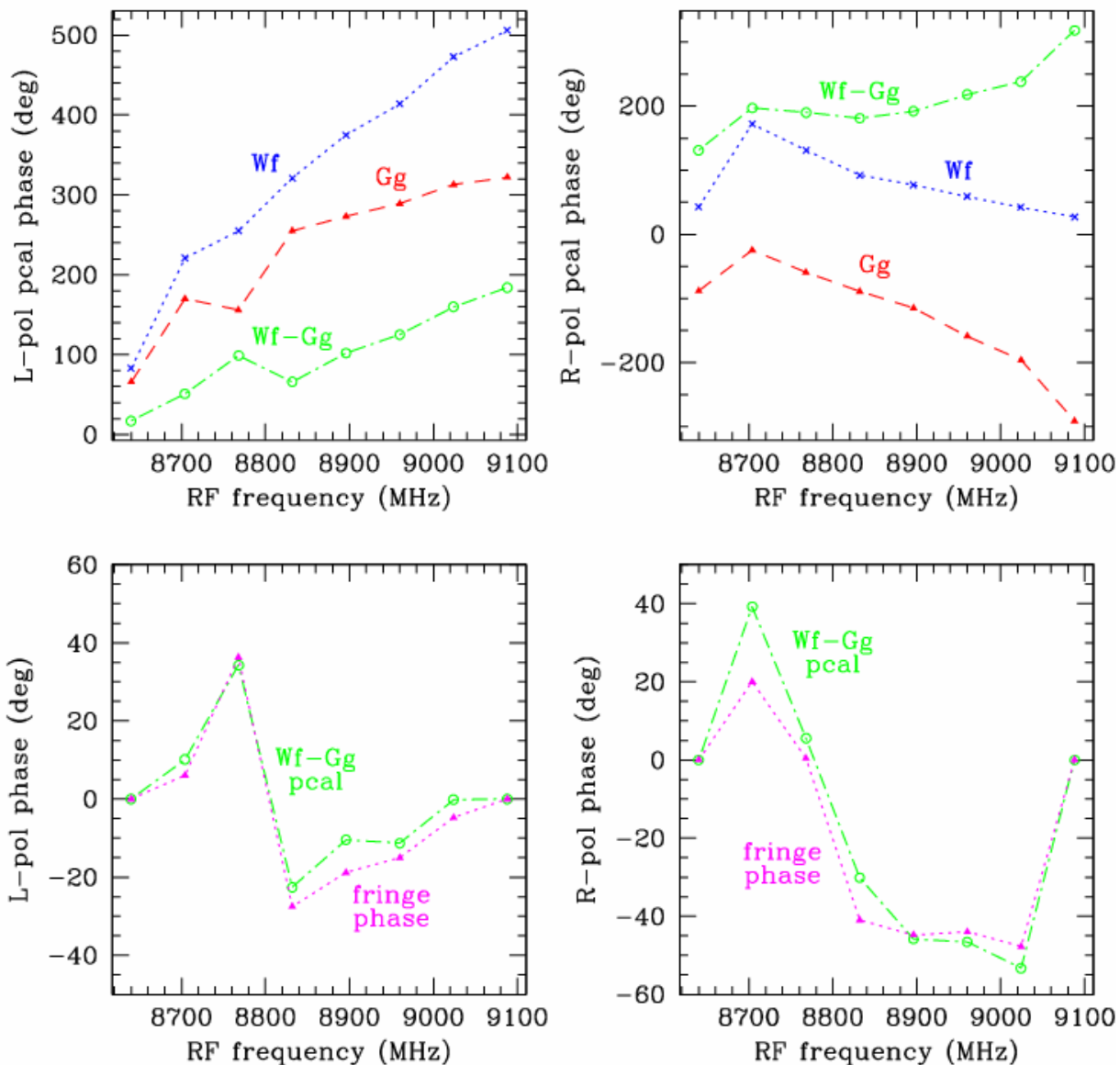


Figure 1. Frequency dependences of phase cal and fringe phases for scan 144-1840, which is typical of the higher-SNR scans. Lefthand panels: L-pol pcal and LL fringe phases. Righthand panels: R-pol pcal and RR fringe phases. Top panels: Westford pcal phase (blue x’s and dotted line), GGAO pcal phase (red triangles and dashed line), and Wf-Gg pcal phase difference (green circles and dot-dash line). Bottom panels: Wf-Gg pcal phase difference (green circles and dot-dash line) and fringe phase when correlator data are fringe-fit using the pcal phases (magenta triangles and dotted line). In order to emphasize the similarities in the frequency dependences of the fringe and differential pcal phases, a straight line (corresponding to a group delay) model, which passes through the first and last frequency points, has been subtracted from each set of eight fringe or pcal phase points, so that the first and last plotted points are identically zero.

The upper panels in figure 1 show the individual station pcal phases, as well as the differences. For ideal broadband systems, the pcal phase frequency dependence should be the same at two stations (aside from a difference in slope caused by different cable lengths), and the shape at one station should be close to a straight line except near filter bandedges. The dip in the Gg L-pol pcal phase for the 3rd frequency point and in the Gg R-pol pcal phase for the last point look anomalous, but there may be problems at Wf as well.

From earlier investigations it's known that pcal tones at harmonics of 4 MHz are prone to contamination from spurious signals, which can cause phase deviations. For the May 23 setup, 4-MHz harmonics at baseband are also 4-MHz harmonics at RF. The baseband tone at 30 MHz, which was extracted at correlation along with the 4-MHz tone and six other tones (all of which are multiples of 4 MHz), is therefore not a harmonic of 4 MHz at either RF or baseband. One might therefore hope that fringing the data with the 30-MHz pcal phases would improve the flatness of the fringe phases. When tested, however, it did not.

For geodetic data we often use “additive phases” to clean up errors in the pcal phases that are constant with time. Such an approach proved not viable for the bbd data. As seen in the lower left panel of figure 2, the multiband (MBD) differences between polarizations within a scan varied significantly over the session, whereas with a properly working phase cal system one would expect much better stability. On the other hand, when the data are fringed with manual phases (i.e., an instrumental correction phase for each channel that is constant over the session), the scatter in the MBD differences is consistent with the standard errors, as shown in the lower right panel of figure 2. The marked improvement in MBD stability in going from normal pcal to manual phase fringing has two implications:

- The Wf and Gg systems, exclusive of phase cal, are highly phase-stable between frequency channels and polarizations.
- The phase stability of the pcal system at one or both stations is poor.

Further information on instabilities in the pcal data is presented later in this memo.

The fact that the fringe phase and pcal difference phase curves in figure 1 are similar means that manual phases that are nearly the same for all frequency channels should yield fringe phases that are flat over frequency. All the results reported here for manual-phase fringing were done with all the manual phases set to zero. This is equivalent to assuming the two systems have identical phase responses, aside from any group delay difference. This assumption proved to be remarkably good. For the seven LL scans with SNR > 40, e.g., the rms variation of fringe phase over frequency is 2-4°, while the theoretical value based on the SNR is 2-3°. The variation is larger for RR due to lower SNR and larger intrinsic variation, but even so, it is several-fold smaller than with normal pcal fringing.

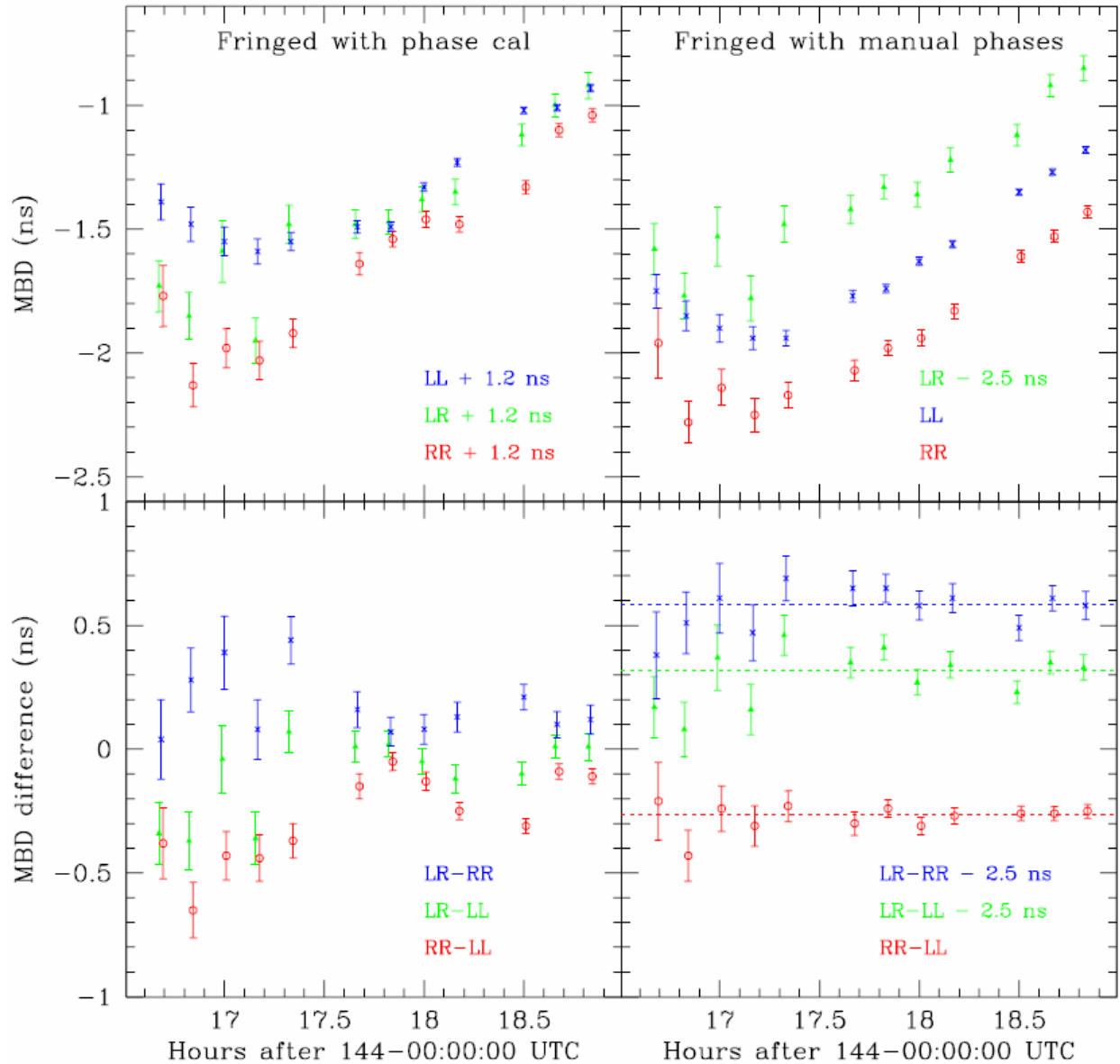


Figure 2. Residual (to correlator model) Wf-Gg multiband delays for LL, RR, and LR (top panels), and the three polarization differences (bottom panels), with the correlator data fringe-fit with phase cal phases (lefthand panels) and with manual phases (righthand panels). Dashed horizontal lines in the bottom right panel are the weighted mean values of the three MBD differences. Constant adjustments of 1.2 or 2.5 ns are made in some cases simply to decrease the vertical spread in the plots.

3. Fringe phases

A further test of the instrumental stability is to compare the fringe phase time series. The top three panels of figure 3 show the LL, RR, and LR fringe phases for the entire session, and the lower two panels show the RR-LL and LR-LL phase differences. The large variations in the undifferenced phases within a scan are probably predominantly atmospheric in origin, although some contribution from the LOs cannot be discounted. The jumps at the scan boundaries occur because the best-fitting delay+rate model found by fourfit changes from scan to scan. The

variability, both within and between scans, is greatly reduced in the phase differences, as is expected, because atmospheric and LO variations should be the same for the two polarizations at each station, and because the fourfit models for different polarization correlations should be close to the same. The small jumps at some scan boundaries (e.g., at 110 minutes in RR-LL) in the phase differences are caused mainly by differences in the singleband delay (SBD) and MBD fourfit solutions. These jumps are almost completely eliminated when the data are fringe-fit so as to maintain constant delay offsets between the polarizations – see figure 4.

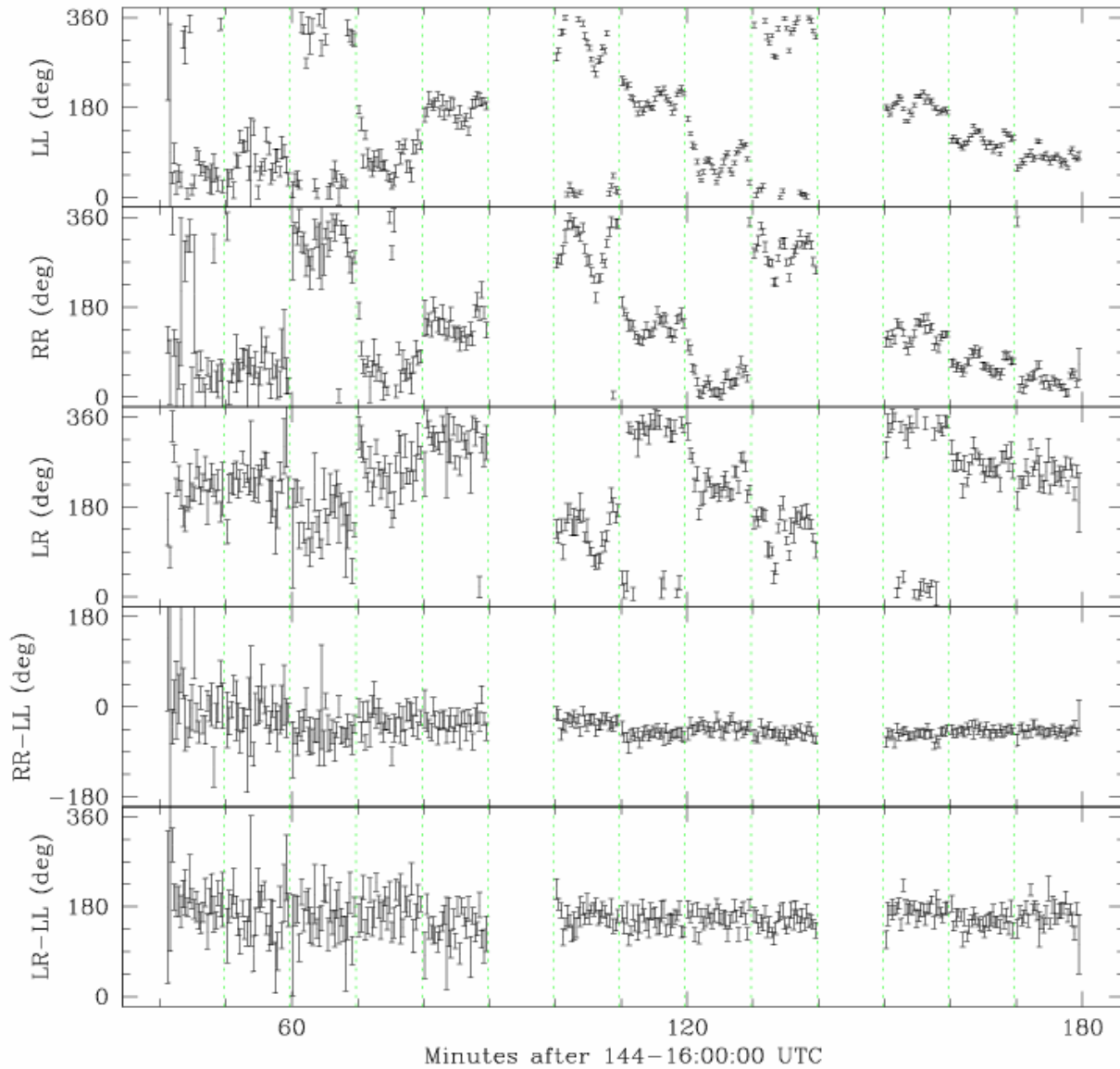


Figure 3. Residual (to correlator+fourfit model) fringe phase time series for data fringe-fit with manual phases (see text). Each point, which is represented by $\pm 1\sigma$ error bars, is a 20-second coherent average. Vertical dashed green lines represent the 10-minute scan boundaries. Top three panels show the LL, RR, and LR phases; bottom two show the RR-LL and LR-LL differences.

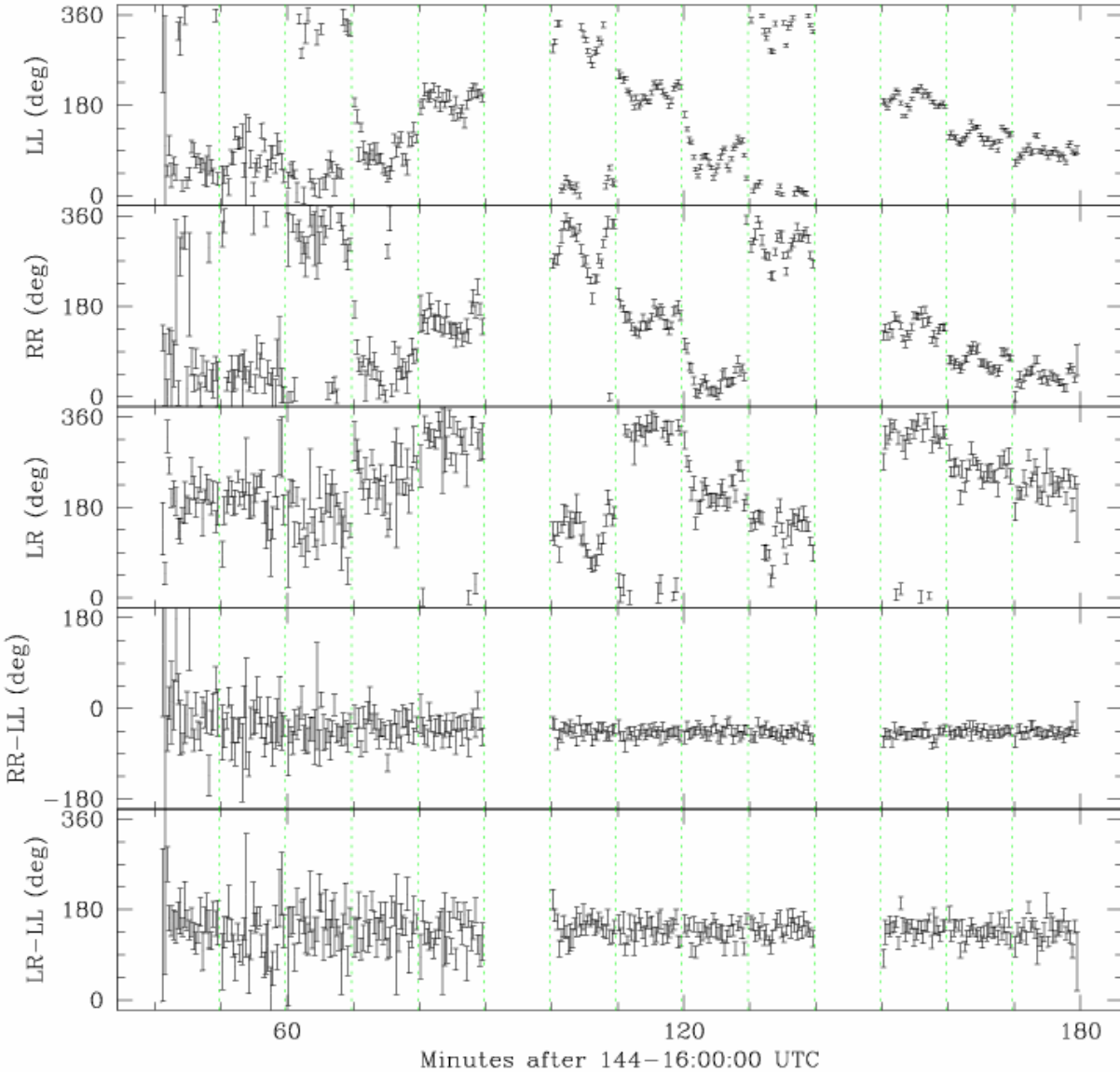


Figure 4. Same as Figure 2 except that additional constraints were applied in the fringe-fitting: (a) residual SBD was forced to zero (when unconstrained, the SBD was between -3 and +4 ns), and (b) MBD for each pol for each scan was set to a specified value close to the unconstrained best-fit value, with the added constraint that the RR-LL and LR-LL MBD differences were held fixed from scan to scan.

4. Fringe amplitudes

Fringe amplitudes and their ratios between polarizations are displayed in figure 5.

The nearly factor-of-two ratio between parallel-hands amplitudes could be caused by SEFD differences, including polarization-dependent RFI effects. If the SEFDs are constant, or if they vary by the same fractional amounts for both polarizations, the RR/LL ratio should be constant, which it nearly is for the last seven scans. The earlier scans have some sort of modulation problem discussed in the next section.

That the LR cross-hands amplitude is as strong as it is relative to the parallel-hands is almost certainly due to the fact that the antenna-source geometries caused the two feeds to be rotated relative to the source by different amounts, so that a radio wave propagating from the source with linear polarization perfectly aligned with the H polarization of one feed, say, was received by the other feed with the polarization plane somewhere between its H and V. For alt-az mounts like Westford and GGAO, this difference in received polarization angle is the parallactic angle difference, which for the bbd test is plotted in the lower right panel of figure 6.

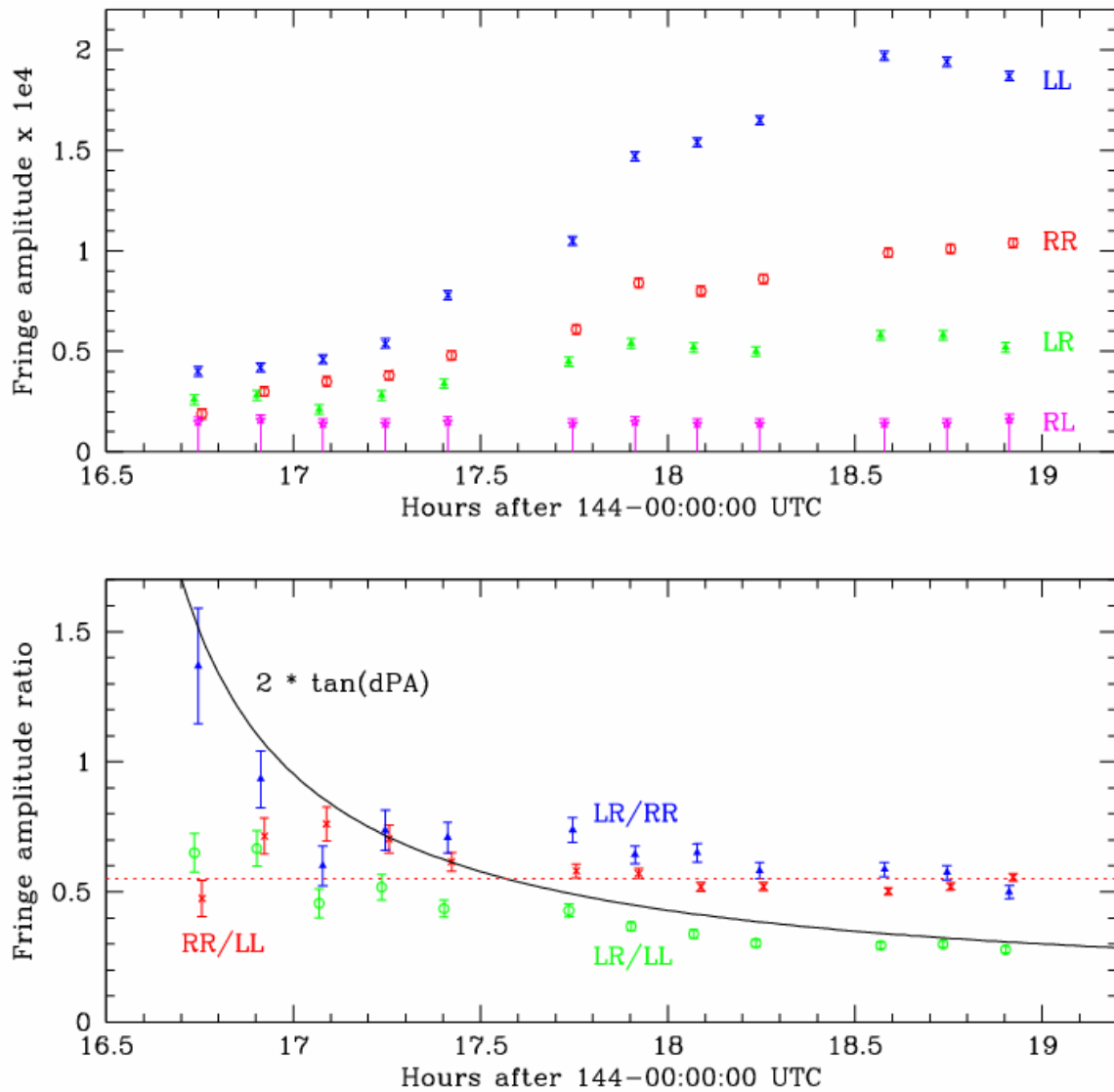


Figure 5. Fringe amplitude (upper panel) and amplitude ratio (lower panel) time series. Error bars are $\pm 1\sigma$ except for RL amplitudes, which are upper limits. Amplitude ratios with RL are not shown since there were no RL detections. Correlator data were fringe-fit with manual phases. Dashed red horizontal line in lower panel at $y=0.55$ is intended only as a reference to judge the constancy of the RR/LL ratio. Solid black curve in lower panel is the expected time dependence of a cross-hands/parallel-hands fringe amp ratio (e.g., LR/RR and LR/LL) due to differential rotation of the feeds at the two sites, under the simplifying assumptions of an unpolarized source and constant SEFDs. (The factor of 2 multiplying $\tan(dPA)$ was introduced simply to raise the curve into the approximate abscissa range of the observed ratios.)

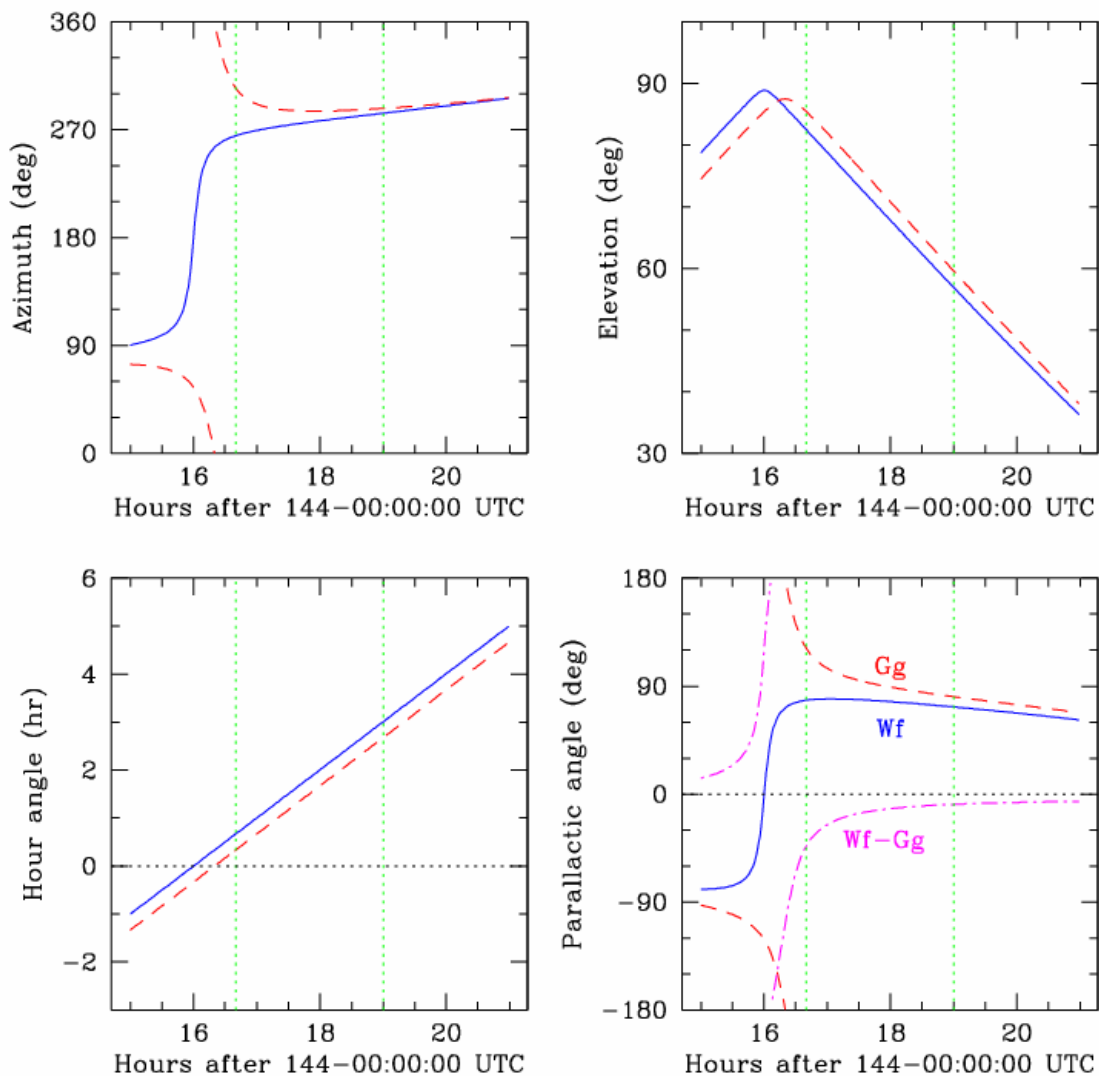


Figure 6. Antenna angles at GGAO (dashed red curves) and Westford (solid blue curves) vs. UT when tracking 3C84 on 2008 May 23. Dot-dash magenta curve in lower right panel is the difference in parallactic angles at the two sites. The two dashed vertical green lines in each panel mark the start and stop epochs of the recorded scans. Because the declination of 3C84 lies between the latitudes of GGAO and Westford, the source transits to the north at GGAO and to the south at Westford. This leads to the rapid changes in the parallactic angles, and in their difference, shortly before observations began.

A simple model for the relationships between the various cross- and parallel-hands amplitudes assumes that the source is unpolarized (which 3C84 nearly is) and that both feeds are aligned identically relative to local vertical/horizontal. The amplitudes may be expressed as:

$$LL = I_f * S_{corr} * |\cos(dPA)| / \sqrt{WfL * GgL}$$

$$RR = I_f * S_{corr} * |\cos(dPA)| / \sqrt{WfR * GgR}$$

$$LR = I_f * S_{corr} * |\sin(dPA)| / \sqrt{WfL * GgR}$$

$$RL = l_f * S_{corr} * |\sin(dPA)| / \sqrt{WfR * GgL}$$

where WfL (WfR) is the L-pol (R-pol) SEFD at Westford,
 GgL (GgR) is the L-pol (R-pol) SEFD at GGAO,
 l_f is a loss factor,
 S_{corr} is the correlated flux density of the source, and
 dPA is the parallactic angle difference between the stations.

These equations may be used in two ways to set bounds on the SEFDs.

First, forming the double ratios (RR/LL) * (RL/LR) and (RR/LL) / (RL/LR) from the above equations and then plugging in values from the last scan in figure 5 gives

$$(RR/LL) * (RL/LR) = WfL / WfR < 0.17$$

$$(RR/LL) / (RL/LR) = GgL / GgR > 1.8$$

Translated from L and R to H and V, the first inequality means that the H SEFD at Wf is >6 times higher than the V. Such a large ratio seems unreasonable. Note that the two inequalities are not independent, as the RR/LL ratio, which is the square root of the product of the two double ratios above, has the well-determined (at least for the last seven scans) value of ~0.55, by the lower panel in figure 5. The fact that RR/LL is not zero rules out extreme “explanations” for the low WfL/WfR ratio such as a disconnected cable in the R-pol signal path somewhere, which would correspond to WfR = ∞.

Second, from the model equations, we also have

$$LR/RR = \sqrt{WfR / WfL} * |\tan(dPA)| > 2.4 |\tan(dPA)|$$

$$LR/LL = \sqrt{GgL / GgR} * |\tan(dPA)| > 1.3 |\tan(dPA)|$$

where the inequalities come from plugging in the limits on the SEFD ratios from step 1. The observed ratios, as plotted in figure 5, do indeed obey these inequalities, at least for the last seven scans. Furthermore, the ratios for those scans decrease over time by roughly the predicted amounts.

It seems then that a self-consistent picture for the time dependence and absolute values of the fringe amplitude ratios can be constructed for the later scans, albeit only if the Wf SEFDs differ drastically for the two polarizations. It’s conceivable that a problem in correlation was instead responsible for the lack of RL fringes. Two facts argue against such a cause: (1) The recording mode and correlator setup were identical to those used for the 2008 January 4 fringe test, in which Westford piped R-pol into both polarization channels, and fringes were obtained for all four polarization products. (Thanks to Mike Titus for pointing this out.) (2) The Westford pcal amplitudes and phases are identical in the RL and RR fringe plots, as are the GGAO amplitudes and phases in the RL and LL fringe plots.

5. Modulation/RFI in early scans

There are two unusual features in the first six scans, up until sometime between 1731 and 1740 UT, after which both features completely disappear:

1. The delay rate spectrum exhibits strong, narrow sidebands spaced ~5.7 ps/s apart around the main peak – see figure 7.

- The pcal phase in every channel at Wf is strongly modulated with a period of almost exactly 20 seconds – see figure 8.

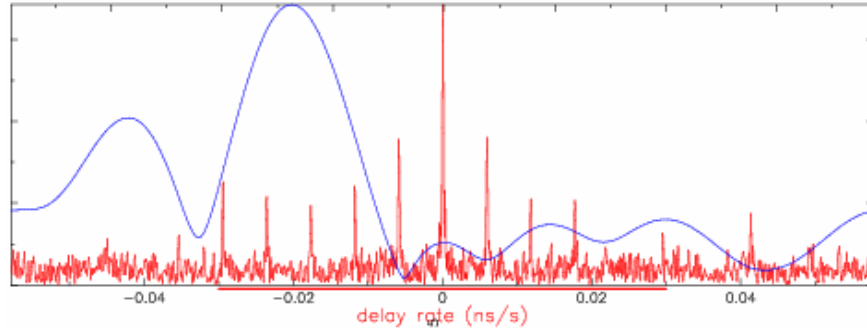


Figure 7. Delay rate spectrum (red) and multiband delay resolution function (blue) from scan 144-1720 LL fringe plot. The narrow rate sidebands on either side of the peak at zero delay rate are spaced ~ 5.7 ps/s apart. The RR rate spectrum for the same scan is very similar. Rate spectra for the four scans before 1720 are also similar, albeit with lower SNR.

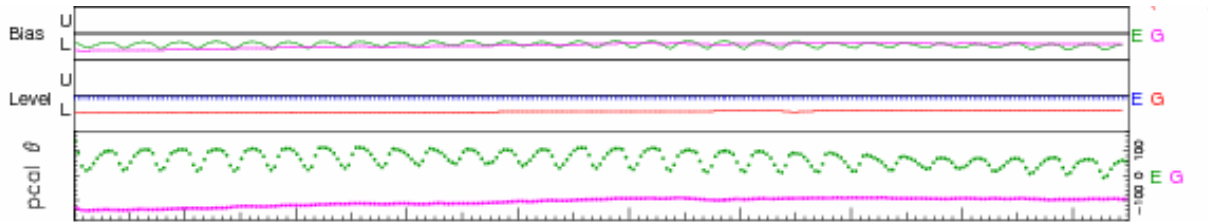


Figure 8. State counts and pcal phase time series for frequency channel X4L from scan 144-1720 LL fringe plot. The upper plot labeled “Bias” shows the fraction of all samples by which positive samples outnumber negative, with an abscissa range from -2 to +2%; Wf is in green, Gg in magenta. The middle plot labeled “Level” gives the fraction of 2-bit data samples in the low-magnitude state, with an abscissa range from 54 to 72%; Wf is in blue, Gg in red. The lower plot shows the pcal phase, with an abscissa range from -180 to $+180^\circ$; Wf is in green, Gg in magenta. The Wf bias, level, and pcal phase plots are nearly identical to the above for the other seven L-pol channels and for the eight R-pol channels of this scan, and for all channels in the preceding four scans. The one exception is that the R-pol levels are close to the optimal value (which is halfway up the plot), unlike the L-pol levels, which are off-scale to the top, which corresponds to too few high-magnitude samples.

If the phase modulation occurred in the LO (as opposed to the RF pcal signal), the downconverted signal from 3C84 would appear at the correlator to have rate spectrum sidebands at harmonics of ~ 5.6 ps/s. The near coincidence in frequency spacing and the complete coincidence in the times when the two features were present convince me that they are of the same origin. But is LO modulation to blame? Note in figure 8 that the bias in the Wf state counts rises and falls by $\sim 1\%$ synchronously with the pcal phase. LO modulation by itself should not affect state counts. Could a bad power supply on an overdriven amplifier cause these effects? If the strength of external RFI varied with a 20-second period (caused by a scanning radar, say), AM-to-PM conversion in an overdriven amplifier could lead to the rate sidebands, and asymmetry in the voltage response to the bias variations. Because the pcal signal is introduced before the feed, both the pcal and quasar signals could become modulated in this way.

6. Phase cal

Figures 9 and 10 show the L-pol pcal amplitudes and phase differences between adjacent channels at the two stations. R-pol shows similar behavior at both stations, except that Wf's R-pol phase variations in channels 1 and 8 are worse than the worst of the L-pol.

Some of the amplitude variations may be due to intra-scan coherence losses that vary from scan to scan. Phase wander on minute and longer time scales within a scan at both stations can cause the coherent average over a scan to vary by 10-20%. Furthermore, the disappearance of the 20-second modulation after 144-1740 could lead to an amplitude increase of ~20% or more. Some channels show a step upward at that time of about this amount, or much more, on top of a gradual increase during the middle part of the session.

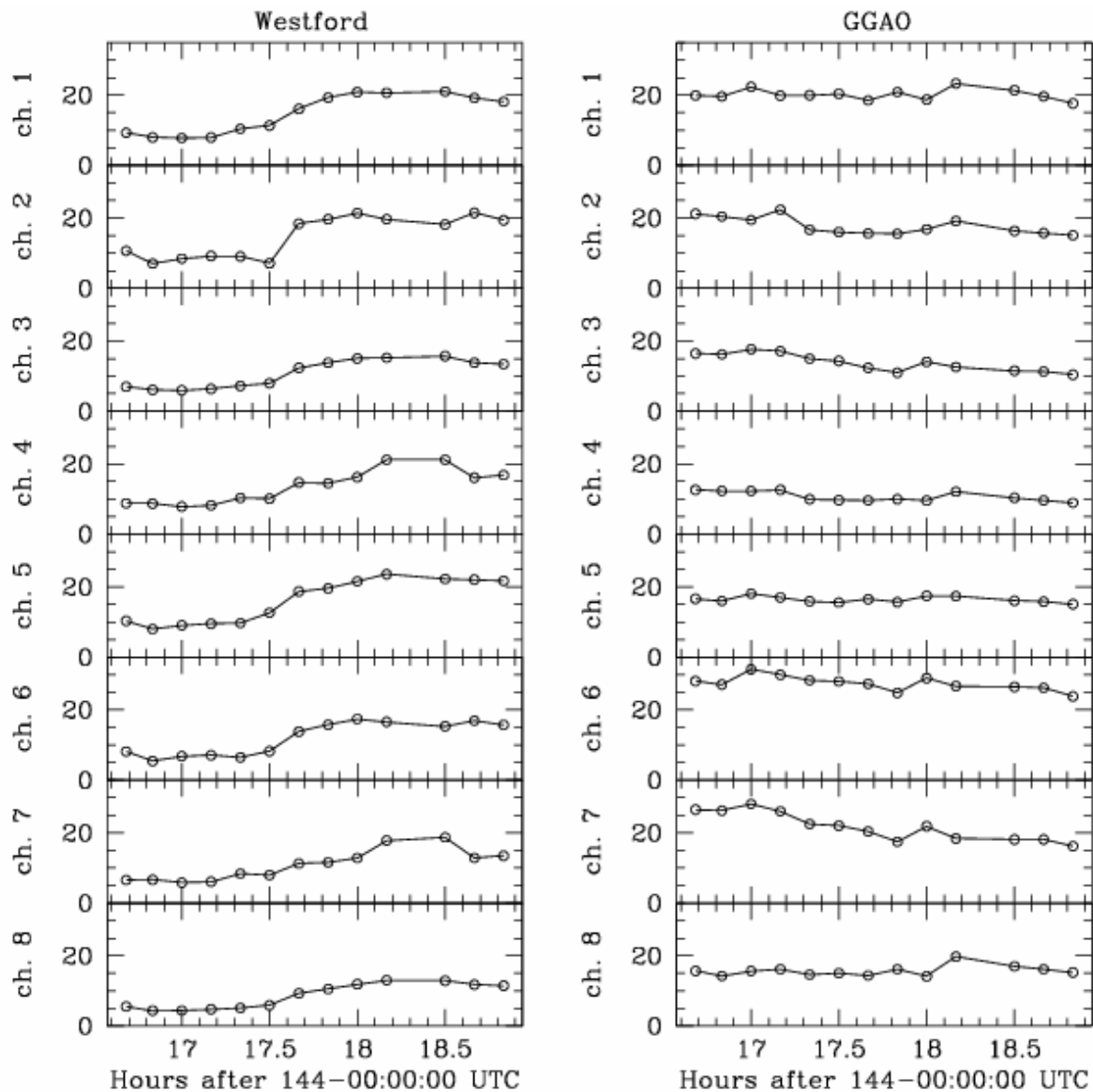


Figure 9. L-pol phase cal amps x1000 as measured at the correlator. Each value is the coherent average over a scan. Coherence losses due to phase wander during a scan will reduce the value compared with an instantaneously measured value.

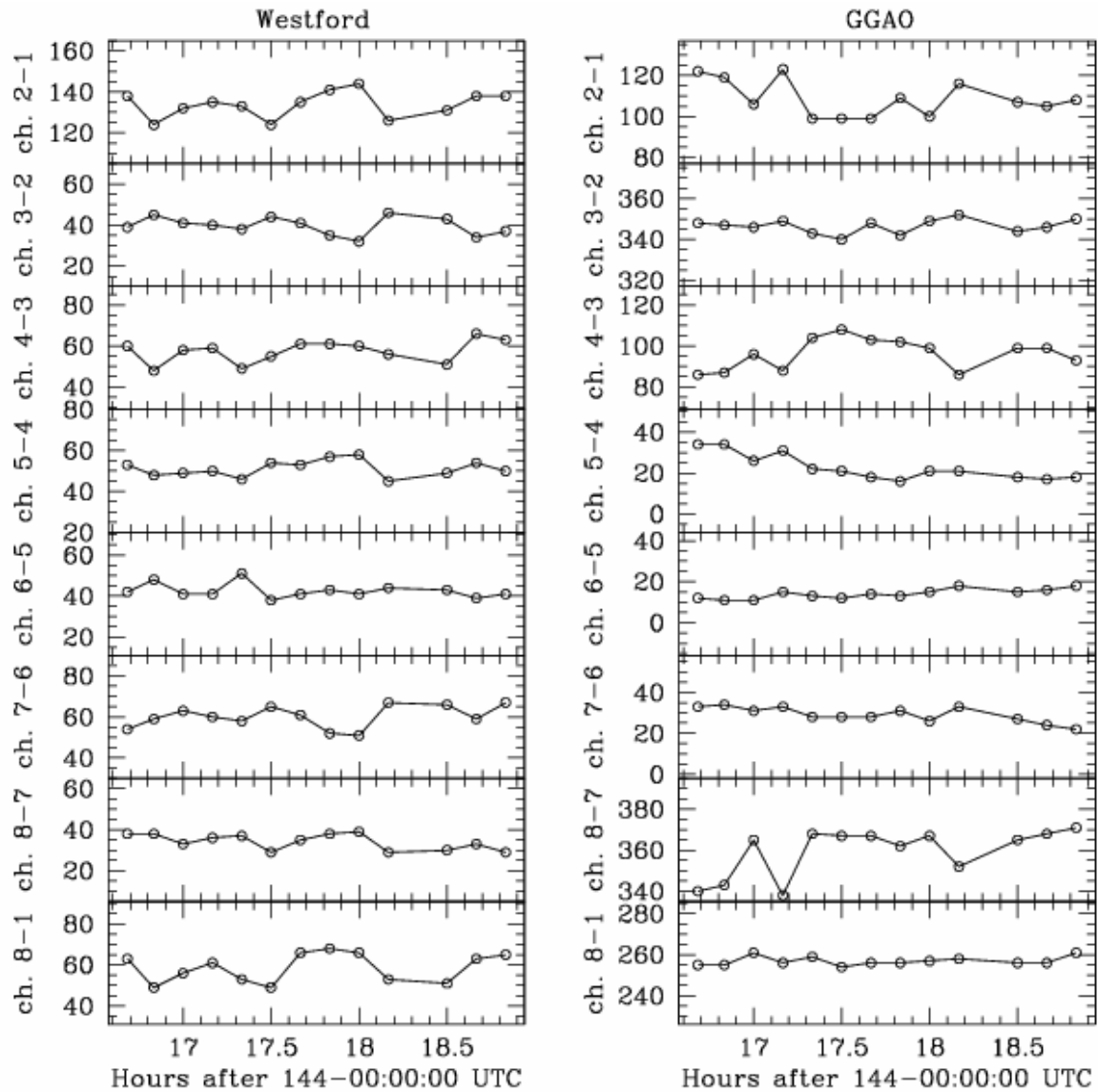


Figure 10. L-pol phase cal phase differences between adjacent frequency channels. Each value is the coherent average over a scan.

The observed pcal phase variations are far larger than expected with properly functioning pcal and DBE systems. The level of variations is larger even than for a typical standard S/X geodetic system with baseband converters whose LO signals are separately phase-locked to the maser. These variations are the cause of the poor stability in polarization-differenced MBDs when the pcal phases are used in the fringe-fitting (cf. figure 2). Spurious signals could be contributing to the instability. The standard tests for spurious signals in correlator data (e.g., plotting pcal amplitude vs. phase) are inconclusive to date, mainly due to the limited range over which the phase changed during the session.